THE ASTROPHYSICAL JOURNAL, 561:L211–L214, 2001 November 10

HARD X-RADIATION FROM A FAST CORONAL EJECTION

H. S. HUDSON
Solar Physics Research Corporation/Institute of Space and Astronautical Sciences, 3-1-1 Yoshinodai, Sagamihara, Kanagawa 229, Japan; hudson@isass1.solar.isas.ac.jp
T. KOSUGI
Institute of Space and Astronautical Sciences, 3-1-1 Yoshinodai, Sagamihara, Kanagawa 229, Japan
N. V. NITTA
Lockheed Martin Solar and Astrophysics Laboratory, 3251 Hanover Street, Palo Alto, CA 94304
AND
M. SHIMOJO
Nobeyama Radio Observatory/NAOJ, Minamimaki, Minamisaku, Nagano 384-1305, Japan
Received 2001 August 25; accepted 2001 October 3; published 2001 October 19

ABSTRACT

We have observed a high-speed coronal ejection in hard X-rays, detectable to an altitude of some 2×10^5 km in the *Yohkoh* 23–53 keV energy bands. Simultaneous imaging at 17 and 34 GHz from the Nobeyama radioheliograph shows complex moving features simultaneous with the ejection, including a compact source that we identify with the rapid X-ray source motion. The hard X-ray and microwave observations agree on ejection velocities in the vicinity of 1000 km s^{-1}. The hard X-ray sources also corresponded in position angle to a bright coronal mass ejection (CME) detected about 15 minutes later and temporally to both fast-drift and slow-drift radio bursts in the decimeter–meter bands. Other components of coronal hard X-ray emission were also detected, including an extended long-duration event with a nonthermal spectrum. We suggest that a major eruptive flare occurred in NOAA Active Region 9415, approximately 26° beyond the west limb at the time of the event. Estimating a source density of 4×10^9 cm^{-3} from the compact source observed at 17 GHz, we find a total electron number (>20 keV) of approximately $N_{20} \sim 1.3 \times 10^{36}$ for the compact part of the source. We infer that these electrons were trapped in expanding loops forming a part of the CME and may have contributed substantial pressure within these loops.

Subject headings: Sun: corona — Sun: flares — Sun: X-rays, gamma rays

1. INTRODUCTION

The solar corona displays many phenomena involving nonthermal particles, which commonly appear during disturbances of different kinds. The techniques of radio astronomy have made it possible to study these accelerated particles since the middle of the 20th century. The meter-wave phenomena (e.g., Wild, Smerd, & Weiss 1963) include types I–V, which variously reveal the presence of global shock waves, relativistic electrons trapped in large-scale magnetic loops, streams of quasi-relativistic electrons escaping the Sun on open field lines, and other remarkable things. Complete physical interpretations of this rich array of phenomena have often proven difficult, however, partly because of the relatively low spatial resolution at radio wavelengths.

Hard X-ray bremsstrahlung provides another means for the observation of such phenomena, but observations have been limited. Without hard X-ray imaging instruments, the best means for observing coronal sources has thus far been to use the solar limb as an occulter. Limb-occulted events have the advantage that bright sources on the solar disk cannot obscure the coronal observations so easily. The pioneering observation in this category was the event of 1969 March 30 (Frost & Dennis 1971), with a microwave counterpart in the form of a remarkable expanding source (Énomé & Tanaka 1971). Subsequent observations revealed other distant over-the-limb events (Hudson 1978; for a review see Cliver et al. 1986). Hard X-ray events from flares inferred to have originated far beyond the limb have tended to have distinguishing characteristics, including long durations, extremely flat spectra, and a lack of thermal soft X-rays.

Yohkoh carries the most sensitive solar hard X-ray imager to date, and it has observed several coronal hard X-ray sources of probably different types (Masuda et al. 1994; Tomczak 1997; Sato 2001). Prior to the observations reported here, however, there have been no studies of *Yohkoh* flares that occurred far beyond the limb, say, by greater than 20° (see Tomczak 2001).

We estimate that the event discussed in this Letter (02:15 UT, 2001 April 18) occurred $27\overset{\circ}{.}3 \pm 2\overset{\circ}{.}3$ beyond the west limb, based on the NOAA reports of Hα flare positions in NOAA Active Region 9415 when it was on the disk. The previous major flare in NOAA AR 9415 occurred at 13:50 UT (*GOES* peak time) on April 15, and from the soft X-ray telescope (SXT) images we find a longitude of W83° for it. The time of the event studied in this Letter corresponds to a position $25\overset{\circ}{.}8$ beyond the limb, within the scatter of the estimate based on Hα flares. Adopting the X-ray position, we estimate an occultation height (altitude of the line of sight) of 8.8×10^4 km. A bright, fast coronal mass ejection (CME) occurred in coincidence, first appearing at 02:30 UT and not visible in the immediately earlier image at 02:06 UT, in the Large Angle and Spectrometric Coronagraph (LASCO) C2 coronagraph on the *Solar and Heliospheric Observatory* (*SOHO*). This Letter reports our detection of rapidly moving hard X-ray and microwave sources in the corona above the presumed flare site, using the *Yohkoh* hard X-ray telescope (HXT) and the Nobeyama radioheliograph.

2. X-RAY OBSERVATIONS

The X-ray time profiles of Figure 1 (*upper panel*) provide a reference time line for the observations. They reveal a disproportionately weak and impulsive soft X-ray emission (*GOES* C2.2). The absence of the usual bright soft X-ray burst following the *Yohkoh* on-board flare trigger signal resulted in a missed observation for SXT, though, so we have no contem-

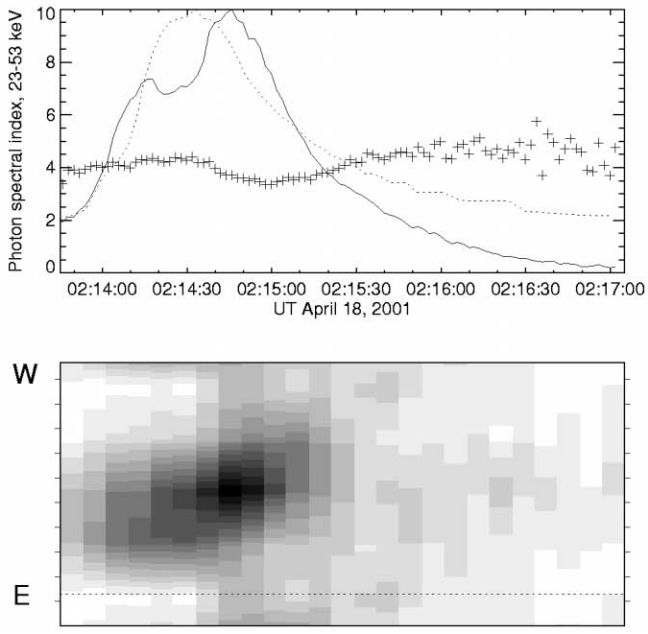

FIG. 1.—*Upper panel*: Variation of spectral index with time during the event. The figure also shows background-subtracted hard X-ray fluxes (23-33 keV) from *Yohkoh* HXT (*solid line*) and soft X-ray fluxes (*GOES* 1–8 Å; *dotted line*) for the event. The X-ray fluxes are normalized to a peak of 10 for each plot; the *GOES* event classification was C2.2, and the peak hard X-ray flux about 57 counts $(\mathrm{cm}^2\ \mathrm{s\ subcollimator})^{-1}$, 23–33 keV. The second hard X-ray peak corresponds to the ejection and has a flatter hard X-ray spectrum. *Lower panel*: Series of one-dimensional hard X-ray images from 5 s integrations in the 23–53 keV band, arranged in a stack plot. The tick marks show intervals of 2×10^4 km and show the east-west position of the source (west at the top). The initial source is stationary and just above the limb (*dotted line*; shown at the north-south position of the moving source).

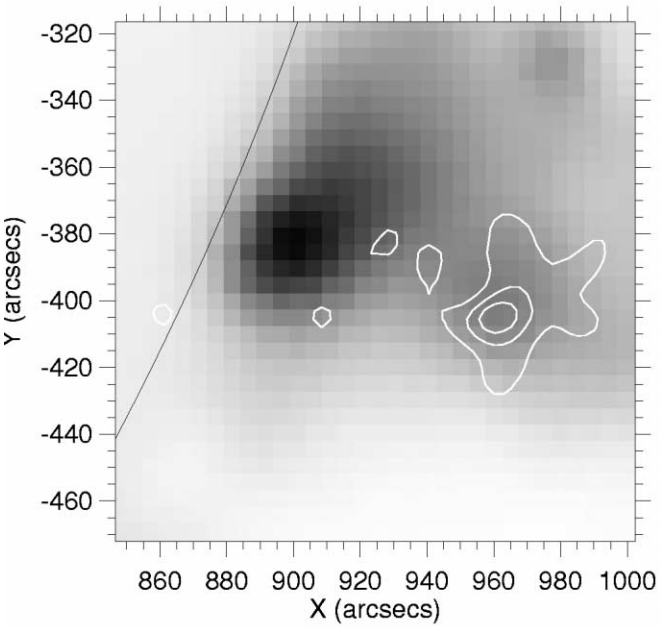

FIG. 2.—Hard X-ray (23–33 keV) contours (40%–80%) superposed on a 17 GHz Nobeyama radioheliograph image at the end of the X-ray imaging observations of the moving source. The radio image is a 1 s snapshot at 02:15:38 UT; the X-rays are integrated over 02:15:33–43 UT. Within uncertainty, the X-ray source matches the location of the moving coronal source, which continues its outward motion as shown in Fig. 3 (*lower panel*). The solid curve at the upper left shows the position of the limb.

poraneous *Yohkoh* images other than those provided by HXT. A weak postburst increase is visible in the *GOES* soft X-rays, consistent with the topmost part of the presumed flare arcade. The hard X-ray images (the 23–53 keV bands) show a source initially appearing along the limb and then moving rapidly outward to the west. The hard X-ray spectrum can be determined approximately from the four energy bands of HXT, and as Figure 1 shows, the statistical errors in the data are small enough to show the hardness variations. The spectrum initially had a photon power-law index of 4.3 over the range ~23–93 keV; in the second peak of Figure 1, the spectral index dropped to 3.4. This second peak corresponds to the moving source.

We have carried out standard maximum entropy method (MEM) deconvolutions of the HXT data but have trouble with convergence given the flux level of the event, which had a peak 23–33 keV rate of 57 $(\mathrm{cm}^2\ \mathrm{s\ subcollimator})^{-1}$; some images look reasonable, but others do not. This is the behavior one would expect for a spatially large source, which could either be intrinsic or the result of smearing induced by rapid source motion. Figure 2 gives an example in comparison with a simultaneous Nobeyama 17 GHz radioheliogram. In order to check the MEM results, we have also used the PIXON technique as available in the *Yohkoh* software (Metcalf et al. 1996). The images thus produced are interestingly different, with much reduced fine structure. This would also be consistent with extended or smeared sources. For each MEM image, we can determine the location of peak brightness, and we show these in Figure 3*a* for the time range up to 02:15:45 UT. The east-

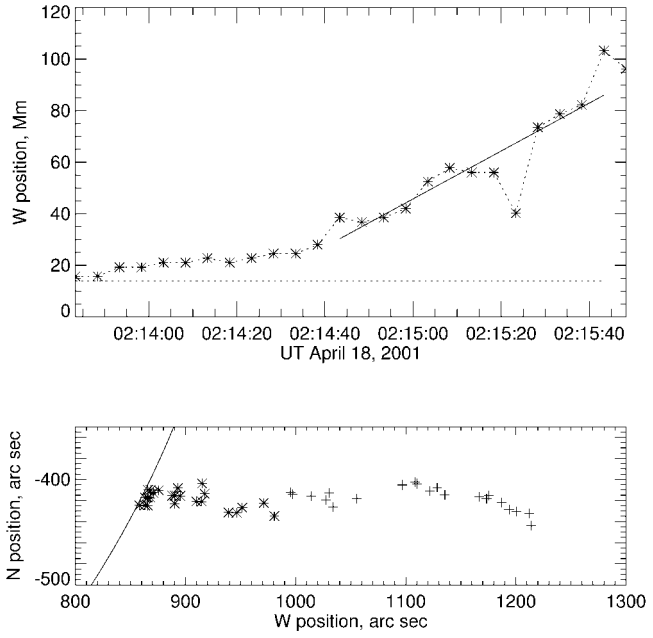

FIG. 3.—*Upper panel*: Height vs. time plot of the east-west peak locations in 5 s integrations of the *Yohkoh* HXT M1 channel (23–33 keV) MEM images. The solid line shows a fit to the peak locations in the time range 02:14:45–02:15:45 UT, and it has a projected velocity of about 930 km s^{-1}. The dotted line at the bottom shows the approximate location of the solar limb. *Lower panel*: Positions of the X-ray peak locations (*asterisks*) together with positions of the compact microwave source (*plus signs*), showing points spaced by 5 s in time starting at 02:15:53 UT. The hard X-ray source remains visible to approximately 100 Mm above the limb and therefore about twice that above the photosphere if the motion is radial, the microwave source to about 3 times the height.

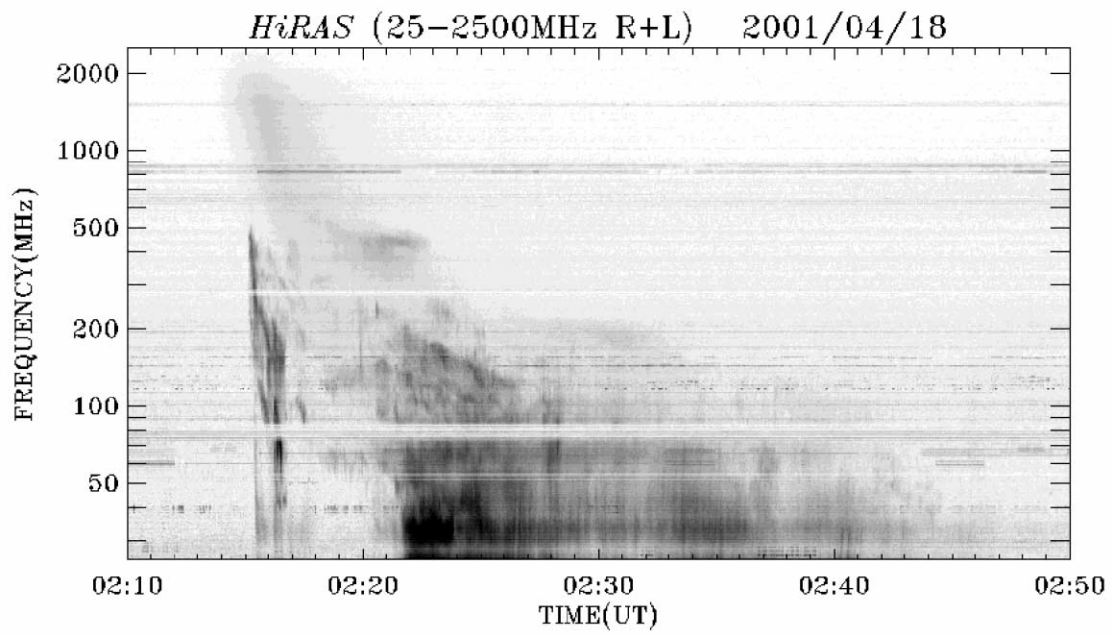

FIG. 4.—Hiraiso spectral observations from the HiRAS spectrometer, plotted with frequency increasing upward rather than wavelength (in this type of plot, downward drifts correspond to motion away from the solar surface due to decreasing density and plasma frequency). One interesting feature to note for this event is the slowly drifting decimetric continuum in the time range 02:15–02:19 UT, approximately the time range of the moving microwave source. The onset time of the type III–like features is 02:14:09 UT at ~440 MHz, based on the Culgoora spectral observations. The type II–like features start at about 02:21 UT at about 200 MHz.

west coordinates initially show little motion, but for the final minute (corresponding with the second peak of the hard X-ray burst) the peak positions increase rapidly, consistent with a motion of about 10^3 km s^{-1}. The MEM image centroids show consistent behavior. After 02:15:45 UT, the inferred locations begin to scatter widely due to lack of convergence, which we attribute to image complexity; the peak flux of this event corresponds to a class M *GOES* event, and it would present no image convergence problems if the image were simple.

The HXT fan-beam elements allow us to confirm the source motion in a rigorous way in spite of the image complexity. Sets of four fan-beam subcollimators of HXT directly form one-dimensional images with a response pattern about 0.′5 wide at half-maximum, in four different fringe orientations (Kosugi et al. 1991). Each fan-beam orientation is thus sampled in four phase steps, so a weighted sum of the four responses generates a simple image covering an angular domain of 2′6″. Most of the spatial resolution of HXT is lost, but source motion can be detected within this field of view. Figure 1 (*lower panel*), shows a stack plot of fan-beam images using the four HXT subcollimators with fringe patterns oriented north-south. This relatively direct observation shows motion consistent with the MEM imaging but with a lower signal-to-noise ratio because of the low effective area of the small number of HXT fan-beam subcollimators. The advantage of the fan-beam images is that they have none of the ambiguity associated with a full HXT image synthesis and require no specific assumptions other than the field-of-view center coordinates, which we have taken from the standard MEM images here. Figure 1 clearly shows image displacement consistent with that of the microwave source (see below) and also displays a sudden expansion just at the onset of the motion. We attribute this to a large-scale source appearing above the limb just at the onset of the second hard X-ray flux peak and the spectral hardening.

3. RADIO OBSERVATIONS

The microwave (17 and 34 GHz) observations of this event shown in Figures 2 and 3*b* are also novel. The microwave sources initially resemble those of a typical soft X-ray ejection, in the form of loops with both perpendicular and parallel motions (e.g., Hudson, Acton, & Freeland 1996; Ohyama & Shibata 1998).

Later, a compact unpolarized blob moves outward, with a projected velocity on the order of 10^3 km s^{-1}, and continues the motion of the X-ray source as shown in Figure 3*b*. This isolated compact source is resolved at 17 GHz, with a brightness temperature T_b falling from $\sim 10^5$ K at 02:15:45 UT to $\sim 10^4$ K at 02:16:45 UT, and appears to separate from the other microwave features at about the end of the interval in which the hard X-ray source is detectable. It is unpolarized and initially has an approximately flat spectrum in flux density, consistent with optically thin free-free emission. By equating the Rayleigh-Jeans law with a standard expression for free-free emission, we have $n_e = (f^2 T_b T_e^{0.5}/0.16l)^{1/2}$. This yields a density $n_e \sim (1\text{–}4) \times 10^9$ cm^{-3} at the time of the last reliable X-ray image of the ejection. Here we take the source depth l to be the square root of the source area at half–peak brightness temperature. This rough estimate assumes unity filling factor and an electron temperature in the range 2×10^4–3×10^6 K, covering the temperature range from prominences to hot active region loops. The position angle of the microwave ejection began at ~230°, consistent with the centroid of the CME at ~245°, as estimated from the LASCO C2 image.

We have used the SOLARSOFT tools to co-align the hard X-ray and microwave images, with the result shown in Figure 2. Due to a temporary loss of the guide star Canopus, this co-alignment required an adjustment of the *Yohkoh* roll angle by −1.°43, as calculated from the known drift rate of the reference

gyro. The compact hard X-ray source coincides with the compact microwave source. This is attractive because the microwave free-free emission requires a relatively high density at the altitude of the hard X-ray emission. To determine the number and spectrum of the nonthermal electrons in this source, we use the Bethe-Heitler approximation of thin-target bremsstrahlung and take the maximal density inferred above. At 02:14:45 UT, we find $N_{20} \sim 1.3 \times 10^{36}$ electrons above 20 keV, corresponding to an instantaneous total particle energy of about 6×10^{28} ergs, for $n_e = 4 \times 10^9$ cm^{-3}. A higher density in the radio source, as, for example, with a nonunity filling factor, would result in a lower estimate. However, this number also represents a lower limit in the sense that electrons can escape from the corona and disappear by precipitation; the propagation timescales could be as short as 1 s, so that a burst 40 s in duration could have a total energy greater than 10^{30} ergs.

Peculiar fast-drift and slow-drift bursts, resembling type III and type II, were observed at the Culgoora and Hiraiso spectrographs, as shown in Figure 4. The bursts began between 02:14 and 02:15 UT, in good coincidence with the microwave and X-ray events, and the starting frequency of the slow-drift burst was greater than 1 GHz as observed at Hiraiso, roughly consistent with harmonic plasma-frequency emission at the density inferred from the microwave spectrum ($\sim 4 \times 10^9$ cm^{-3}). The associated type III burst has a starting frequency of about 440 MHz, which would correspond to lower densities (6×10^8–2.4×10^9 cm^{-3}, depending on the emission harmonic).

4. CONCLUSIONS

We have observed a rapidly moving hard X-ray source relatively high in the corona, at inferred altitudes ranging to about 2×10^5 km, in association with sources observed at 17 and 34 GHz in free-free emission. At meter waves, the hard X-ray source followed a fast-drift burst and coincided with a slow-drift decimeter/meter-wave source with some features of a type II burst. The hard X-ray spectrum and duration differ from those previously observed in extreme over-the-limb events; this is the first imaging observation in hard X-rays of such a coronal source, and we do not know if the motions detected are typical. The hard X-ray emission is almost certainly identifiable with one or the other of the microwave and meter-wave phenomena observed simultaneously, and with some component of the CME. We find that the hard X-ray emission, even at this great altitude, may require a total electron energy content as great as 1% of the total energy of a class X flare. The source volume at 02:15:45 UT is about 1.5×10^{29} cm^{-3}. This implies that the nonthermal electrons above 20 keV represent a tail population on the order of 0.05%, with an energy fraction of about 3%. Taken as a whole, the observations suggest that we are observing electrons trapped in expanding loops, of the type frequently observed in solar flares by SXT (Hudson et al. 1996; Ohyama & Shibata 1998; Nitta & Akiyama 1999) and consistent with the pattern of *U*-burst development sometimes seen at meter wavelengths (Leblanc, Poquérusse, & Aubier 1983).

NASA supported this work under contract NAS8-40801. *Yohkoh* is a mission of the Institute of Space and Astronautical Sciences (Japan), with participation from the US (NASA) and UK (PPARC). We thank the Culgoora Solar Observatory, the Hiraiso Radio Spectrograph, and the *SOHO*/LASCO experiment for their Web-based data services and are grateful to J. Sato for advice and for information on the 1998 April 23 event. Finally, we thank the referee, K. Phillips, for helpful comments.

REFERENCES

Cliver, E. W., Dennis, B. R., Kiplinger, A. L., Kane, S. R., Neidig, D. F., Sheeley, N. R., Jr., & Koomen, M. J. 1986, ApJ, 305, 920
Énomé, S., & Tanaka, H. 1971, in Solar Magnetic Fields, ed. R. Howard (Dordrecht: Reidel), 413
Frost, K. J., & Dennis, B. R. 1971, ApJ, 165, 655
Hudson, H. S. 1978, ApJ, 224, 235
Hudson, H. S., Acton, L. W., & Freeland, S. L. 1996, ApJ, 470, 629
Kosugi, T., et al. 1991, Sol. Phys., 136, 17
Leblanc, Y., Poquérusse, M., & Aubier, M. G. 1983, A&A, 123, 307
Masuda, S., Kosugi, T., Hara, H., Tsuneta, S., & Ogawara, Y. 1994, Nature, 371, 495
Metcalf, T. R., Hudson, H. S., Kosugi, T., Puetter, R. C., & Piña, R. K. 1996, ApJ, 466, 585
Nitta, N., & Akiyama, S. 1999, ApJ, 525, L57
Ohyama, M., & Shibata, K. 1998, ApJ, 499, 934
Sato, J. 2001, ApJ, 558, L137
Tomczak, M. 1997, A&A, 317, 223
———. 2001, A&A, 366, 294
Wild, J. P., Smerd, J. F., & Weiss, A. A. 1963, ARA&A, 1, 291